

# High purity silicon whiskers extraction from silica by novel simple technology

Valeriya S. Kudyakova (✉ [kudyakova@ihim.uran.ru](mailto:kudyakova@ihim.uran.ru))

Russian Academy of Sciences

Elizaveta M. Vagizova

Ural Federal University

Roman A. Shishkin

Russian Academy of Sciences

---

## Research Article

**Keywords:** Chemical vapor deposition, silicon, nanowhiskers, scanning electron microscopy

**Posted Date:** October 14th, 2022

**DOI:** <https://doi.org/10.21203/rs.3.rs-2103235/v1>

**License:** © ⓘ This work is licensed under a Creative Commons Attribution 4.0 International License.

[Read Full License](#)

---

# High purity silicon whiskers extraction from silica by novel simple technology

Valeriya S. Kudyakova<sup>1</sup>, Elizaveta M. Vagizova<sup>2</sup>, Roman A. Shishkin<sup>1</sup>

<sup>1</sup> *Institute of Solid State Chemistry, Ural Branch, Russian Academy of Sciences, Ekaterinburg 620990, Russia*

<sup>2</sup> *Institute of Physics and Technology, Ural Federal University, Ekaterinburg 620002, Russia*

## Abstract

Si dendrites and whiskers were obtained by interaction of gaseous AlF with SiO<sub>2</sub> during transport chemical reaction, using Al, AlF<sub>3</sub> and SiO<sub>2</sub> as starting materials. The dependence of the reaction yield on such technological parameters as temperature, transport gas flow-rate, reactor chamber pressure and molar ratio of the initial compounds was determined. The thermodynamic simulation of processes in reaction chamber was performed by the HSC Chemistry program using HSC-Reaction and HSC-Gibbs modules. Reaction products were characterized by X-ray powder diffraction and scanning electron microscopy. Obtained Si crystallizes as dendrites and whiskers with diameters varying in 100 nm – 24 μm range. The obtained data shows perspectives for adaptation of the proposed technology for production of Si anode material; moreover, the mechanism of proposed synthesis method can be improved for one-stage production of Si/C composite by using CO<sub>2</sub> in process as C source as well as development of a novel CO<sub>2</sub> utilization technology.

**Keywords:** Chemical vapor deposition; silicon; nanowhiskers; scanning electron microscopy

## Corresponding author

Valeriya S. Kudyakova  
Institute of Solid State Chemistry  
Ural Branch, Russian Academy of Sciences  
Ekaterinburg 620990, Russia  
Fax: +7 343 3744495  
E-mail: [kudyakova@ihim.uran.ru](mailto:kudyakova@ihim.uran.ru)

## 1. Introduction

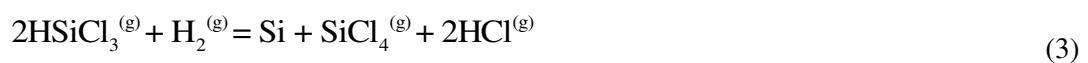
High valuable combinations of the physical and chemical properties, as well as abundant availability, make silicon the key element of nowadays electronics. Besides conventional ways of the silicon application, the novel approaches to use silicon outstanding properties are intensively studied, involving lithium-ion batteries anodes elements; gas adsorption, catalysis, controlled drug delivery and chemical storage [1]. For all mentioned application there are unique features of the silicon processing and requirements for the purity, size and shape of the particles, its surface modification etc.

Specifically, silicon has been demonstrated as the high-capacity anode material of *ca.* 4200 mA h g<sup>-1</sup> based on fully alloyed form of Li<sub>22</sub>Si<sub>4</sub>, but it suffers from dramatic volume changes during the charge and discharge processes, which leads to various issues such as the cracking and fracture of Si particles, formation of an unstable solid electrolyte interphase on the Si surface, and consequently causes rapid capacity degradation of the cell during a cyclical process. The compromise is the Si/C composites which can realize a favorable combination of high specific capacity of Si and mechanical durability of C. These composites can be realized into four categories, including core-shell structure, yolk-shell structure, porous and embedding structure [2]. The other approach to increase the stability of silicon-based anode materials is the use of nanosized structures, since the increase in volume during lithiation of nanoparticles with a size within 1 μm is reduced compared to larger particles [3, 4]. Nanostructures able to withstand the strain caused by a change in the volume of silicon anodes upon introducing lithium without deteriorating the electrochemical properties of the electrode include nanowires [5–11], nanofibers [12–15], nanotubes [12, 14–18] and thin films [19–26].

Nowadays, conventional industrial way of the technical silicon production is carbothermal reduction of the silica [27]:



Nonetheless, chemical purity of such silicon is not sufficient for high-tech applications. Thus, Si suitable for application in lithium-ion batteries (LIBs) as well as in semiconductor and solar technologies is conventionally produced by Siemen's process purification, consisting of the formation and decomposition of the trichlorsilane on inverse U-shape hot filament [28]:



Formation of toxic and corrosive chlorosilanes and hydrochloric acid make this method harmful for environment and challenging hardware design. Hence, the alternative approaches are being developed for silicon purification, which involves fusion, refusion and solidification-

controlled processes. But despite serious research efforts metallurgical approaches is still in the development phase [29].

Synthesis of silicon nanostructures, such as nanoparticles [30,31], hollow silicon spheres [32,33], silicon nanowires [7], silicon nanotubes [14], three-dimensional porous silicon [34,35], and silicon in composites with carbon or oxides [36,37] as the anode material of LIBs has been attracted much attention recently. Such methods as supercritical fluid-liquid-solid (SFLS) synthesis [38], laser ablation or simple evaporation [39], the chemical vapor deposition (CVD) using  $\text{SiCl}_4/\text{SiH}_4$  as starting material [40,41] are investigated to obtain Si nanostructures. However, these state-of-the-art techniques still cannot meet the requirement of commercial applications in large-scale industrial production. Hence, despite the common use of silicon in up-to-date industry, researching new technologies that increases the economic efficiency of the synthesis process and allows silicon to be produced silicon of the desired morphology and structure is still a challenge.

It was found that the chemical transport reactions through aluminum subhalide formation applied in high purity aluminum and aluminum nitride synthesis has a great potential. The major strengths of such approach are [42]:

- relatively low synthesis temperatures (900 – 1100 °C);
- the opportunity to use starting materials (Al and AlN) of technical grades;
- no harmful emissions and environmental safety;
- the opportunity to obtain final product with high purity and in the nanostate.

Moreover, aluminum monofluoride is known to be a strong reducing agent that could react with silica with formation of silicon during CVD. At the same time it is inactive in relation to alumina and, herewith, there aren't strict requirements for initial silica grade - the pure silicon could be synthesized even from chamotte or other silica containing minerals. But only a few information about silicon CVD through aluminum monofluoride transport reaction is published to date [42].

In such a way in the present study a novel method of the one stage CVD synthesis of the silicon dendrites with diameters reaching 100 nm from  $\text{SiO}_2$  by means of chemical vapor transport reaction with AlF is presented. This method involves using fluorides what is not environmentally friendly, but as fluorides acts as transport agent, the process can be organized without its emission into the atmosphere.

## **2. Materials and methods**

High purity Al ingot (99.92%),  $\text{AlF}_3$  anhydrous powder (99.9%) and technical grade  $\text{SiO}_2$  powder (97.0%) were used as a starting materials. Al ingots and  $\text{AlF}_3$  were mechanically mixed in agate mortar for 30 minutes and placed in 5 ml corundum boat ( $\text{Al}_2\text{O}_3$  99%,  $\text{TiO}_2$  0.7%,  $\text{SiO}_2$

0.3%). The second 13 ml boat was filled with SiO<sub>2</sub> powder. Corundum boats were loaded at 5 cm from each other into the middle of a graphite tube, which was placed inside a quartz tube reactor located in laboratory horizontal tube furnace (Fig. 1). The graphite tube is used to prevent the interaction of AlF<sub>3</sub>, forming during the synthesis, with tube reactor material. The reactor chamber was vacuumed by the Value VRD-24 vacuum pump and filled with commercially available 99.9998% argon. The purge of the system was carried out three times to remove impurities of oxygen from the reactor chamber.

The furnace was heated up with a constant rate of 5 °C/min. The vacuum pump created a desirable gas pressure when the operating temperature was reached. The Ar flow was set by the flowmeter MV-304 with precisely controlled rate. The synthesis was performed during the 30-120 minutes and after that the furnace was cooled freely to the room temperature. The Ar pressure was kept at 0.14 MPa level during the cooling to prevent the oxidation of the reaction products. The series of experiments were carried out with different operating conditions (Table 1). The reaction (silicon) yield was calculated as ratio of Si obtained to the theoretical value, calculated from stoichiometry.

Table 1 – the experiments conditions for silicon synthesis

№	T, °C	Chamber pressure, bar	Molar ratio n <sub>Al</sub> /n <sub>AlF<sub>3</sub></sub>	t, min	Argon flow, l/min
1	1100	0.50	4:1	60	0
1	1100	0.10	4:1	60	0
2	1100	0.01	4:1	60	0
3	1000	0.01	2:1	60	0
4	1000	0.01	6:1	60	0
5	1000	0.01	4:1	30	0
6	1000	0.01	4:1	90	0
7	1000	0.01	4:1	120	0
8	1000	0.01	4:1	60	0.1
8	1000	0.01	4:1	60	0.2
9	1050	0.01	4:1	60	0
10	1100	0.01	4:1	60	0
11	1100	0.01	6:1	120	0.1

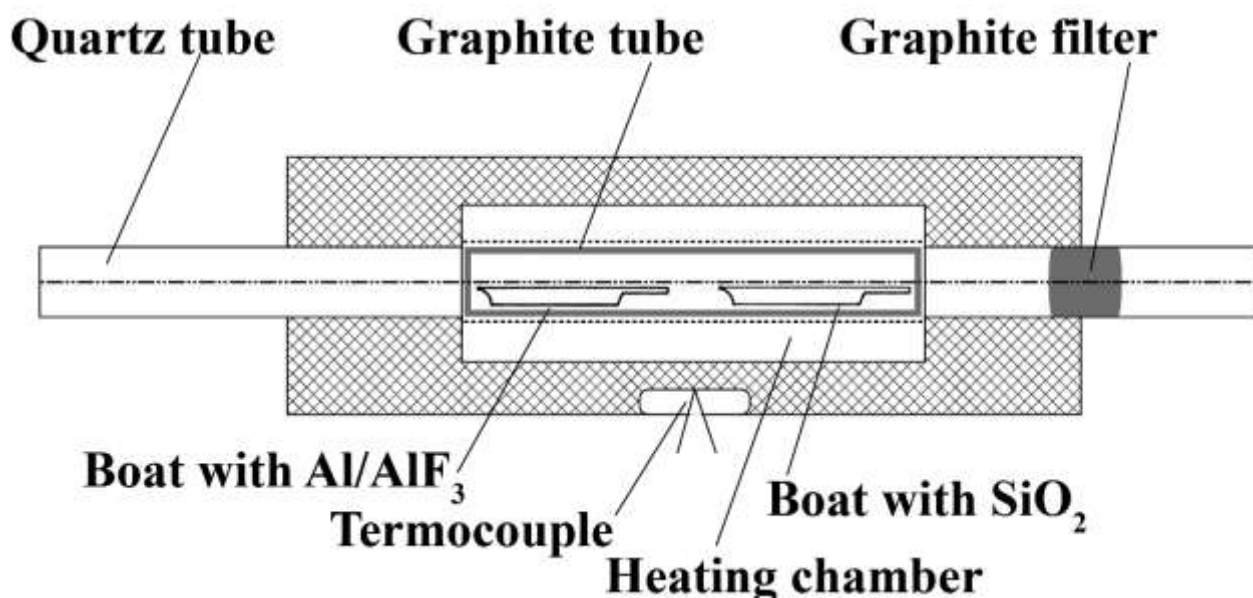


Figure 1 – Schematic representation of the experiential apparatus

The same tube reactor was also used for study of the AlF<sub>3</sub> sublimation rate under different temperature and pressure conditions: the AlF<sub>3</sub> was loaded in 5 ml calcined corundum boat and weighted before and after heating. The pressure was controlled by vacuum valve.

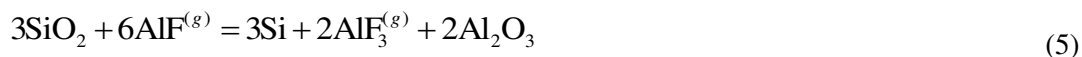
The synthesis products were identified by XRD (XPERT Pro MRD, Panalytical). The morphology of the Si particles and its chemical composition were examined with a Jeol JSM 6390 scanning electron microscope (SEM) and field emission Tescan MIRA 3 LMU electron microscope equipped with a module for energy-dispersive X-ray spectroscopy analysis (EDX).

The thermodynamic simulation was performed by the HSC Chemistry v.9.5 program using HSC-Reaction and HSC-Gibbs modules.

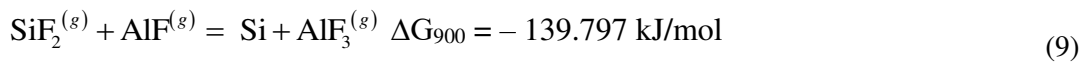
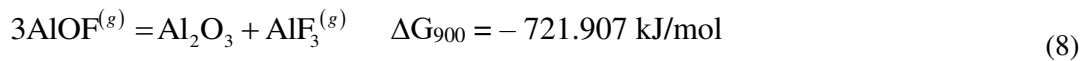
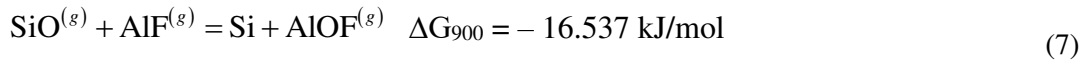
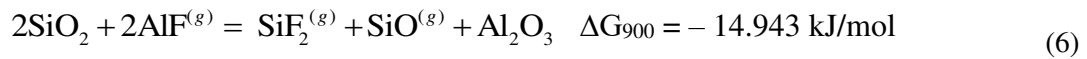
### 3. Results and discussion

#### 3.1. Thermodynamic simulation

The synthesis is based on the following reactions:



One can note that reaction (5) is only formal and does not characterize the synthesis processes completely, since according to the chemical kinetics law there are no reactions with a molecularity higher than three. On the other hand, understanding the kinetics of the synthesis process is important for selecting the optimal technological parameters. Based on the Gibbs free energy values of low-molecular chemical interactions, we proposed a mechanism of silicon formation, consisting of 4 stages (6-9):



The first stage reaction involves 4 molecules, which contradicts the laws of chemical kinetics. We assume that it proceeds with the participation of intermediate metastable compounds not presented among the known thermodynamic data.

Equilibrium compositions of all stages of Si formation as function of temperature at atmospheric pressure are presented at Fig. 2.

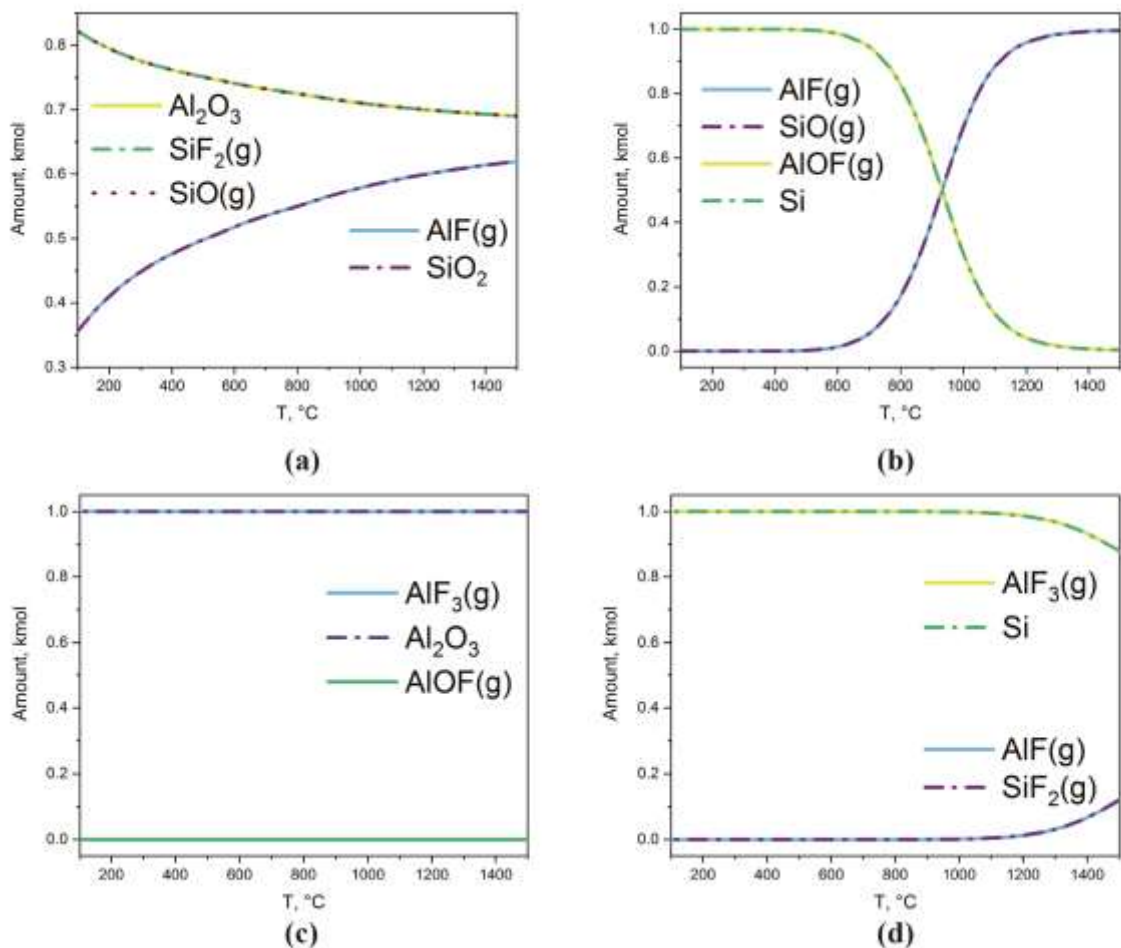


Figure 2 – Equilibrium compositions of all stages of Si formation as function of temperature at atmospheric pressure

Two main processes were simulated in order to select technological parameters: formation of aluminum monofluoride, which acts as a transport agent, and Si formation. Such wise, Fig. 3 represents an equilibrium composition of reaction (4) in dependence of temperature

at various gas phase pressures. The diagram shows that interaction between Al and  $\text{AlF}_3$  starts at temperature range 800-1000 °C and conversely depends on the gas phase pressure. So it is preferably to carry out the reaction (4) is in near-vacuum conditions to provide considerable operating temperature drop.

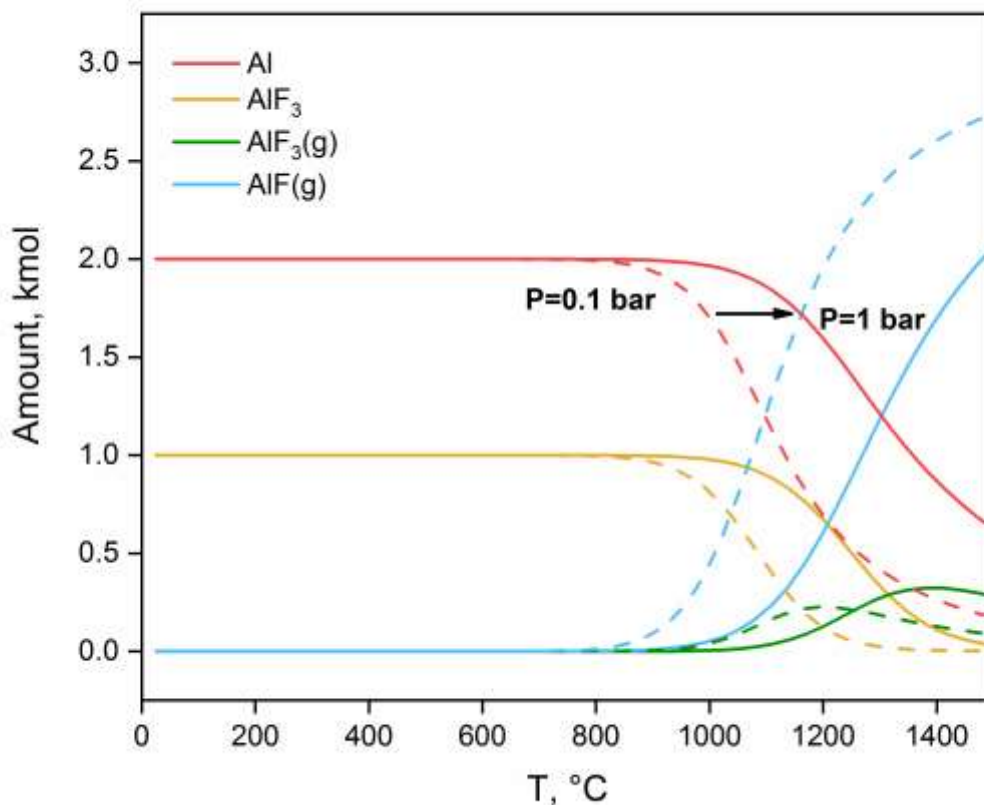


Figure 3 – The “Al-AlF<sub>3</sub>-AlF” system equilibrium compositions

The second major technological step is silicon CVD. The equilibrium composition of the heterogeneous system simulating conditions of this process was calculated on the assumption of stoichiometric amounts of starting materials.

The formation of silicon and aluminum fluorides noticeably affects the silicon yield at temperatures more than 1100°C at 0.1 bar gas phase pressure (fig 4a-b) and the higher the gas phase pressure the higher temperature of silicon fluoridation. From the other hand, the silicon formation cannot start at temperatures lower than temperature of AlF formation, because it is aluminum monofluoride which reduces silicon from dioxide. As described in experimental part, the boat with mixture of Al and  $\text{AlF}_3$  placed separately from the boat with  $\text{SiO}_2$  and direct interaction between Al and  $\text{SiO}_2$  with Si formation is impossible. Nevertheless, this reaction can't be excluded from simulation in HCS Chemistry software, so we present diagrams with



initial temperature 900 °C, which is approximately corresponds to the temperature of AlF formation. It is also proved by experiment because AlF rapidly appears at temperatures more than 900°C at 0.1 bar (fig. 3).

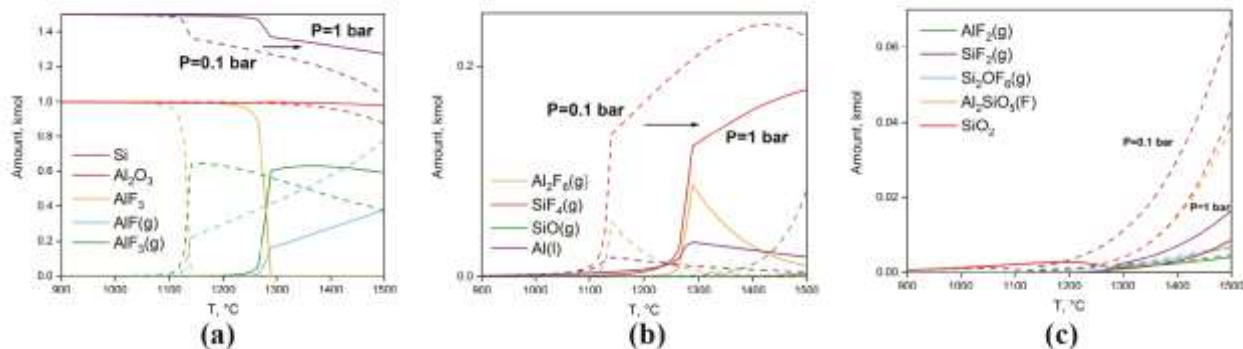


Figure 4 –The system “Ar (g) –AlF<sub>3</sub> (solid) –AlF<sub>3</sub> (gas) – Al (solid) – Al (liquid) – SiO<sub>2</sub>” equilibrium composition: (a) main products; (b) minor products; (c) trace products

It was found that silicon yield drops at the gas phase pressures lower than 0.1 bar (fig. 5a) at 1100°C. Meanwhile there are no changes in synthesized silicon amount until low pressures at 900 °C (fig. 5b).

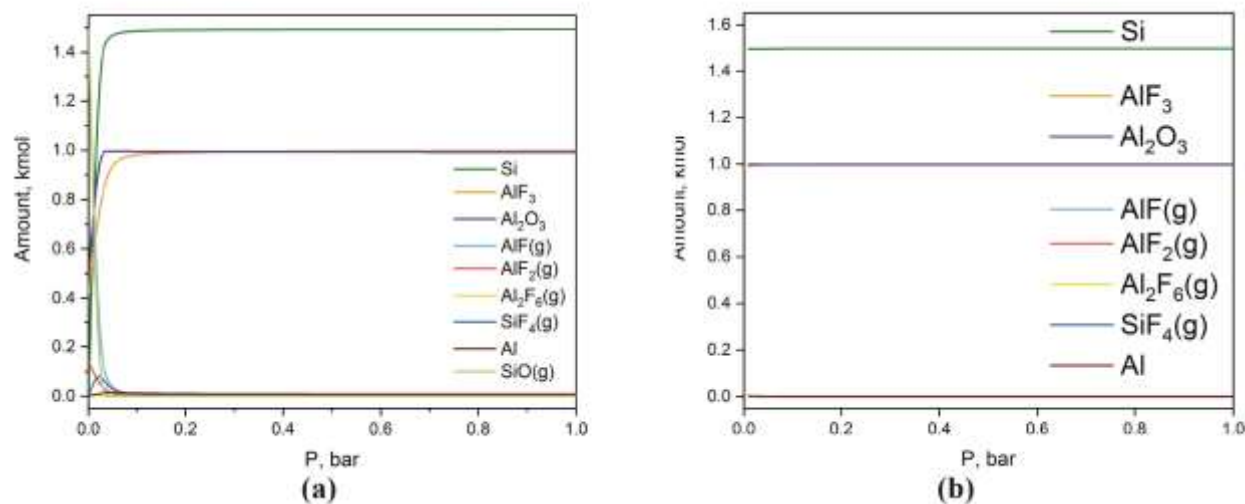


Figure 5 – The system “Ar (g) –AlF<sub>3</sub> (solid) –AlF<sub>3</sub> (gas) – Al (solid) – Al (liquid) – SiO<sub>2</sub>” equilibrium composition at **a.** 1100 °C and **b.** 900 °C

Thus, the two oppositely directed processes are observed in the silicon CVD: AlF formation which intensifies with temperature growth and the gas phase pressure decrease and silicon deposition, with maximum yield at relatively low temperatures and high pressures. So, the most advantageous synthesis parameters from our point of view are operating temperature range 900-1100 °C and pressures 0.01-0.1 bar.

### 3.2. Gas-phase synthesis

The process productivity mainly depends on the aluminum monofluoride formation rate, which is produced within the contact of subliming  $\text{AlF}_3$  and aluminum melt. As the  $\text{AlF}_3$  sublimation rate significantly affects the synthesis process, influence of such synthesis parameters as temperature and pressure in reactor chamber were determined (Fig. 6). The sublimation rate ( $G$ ) was calculated as follows: mass of  $\text{AlF}_3$  which was lost per second from  $1 \text{ cm}^2$ . The aluminum trifluoride sublimation rate drastically rises with the gas phase pressure decrease and temperature growth. It correlates well with the results of thermodynamic simulation of  $\text{AlF}$  formation process (fig. 3). The  $G$  value considerably gains only after  $1000 \text{ }^\circ\text{C}$  that compresses the considered temperature range.

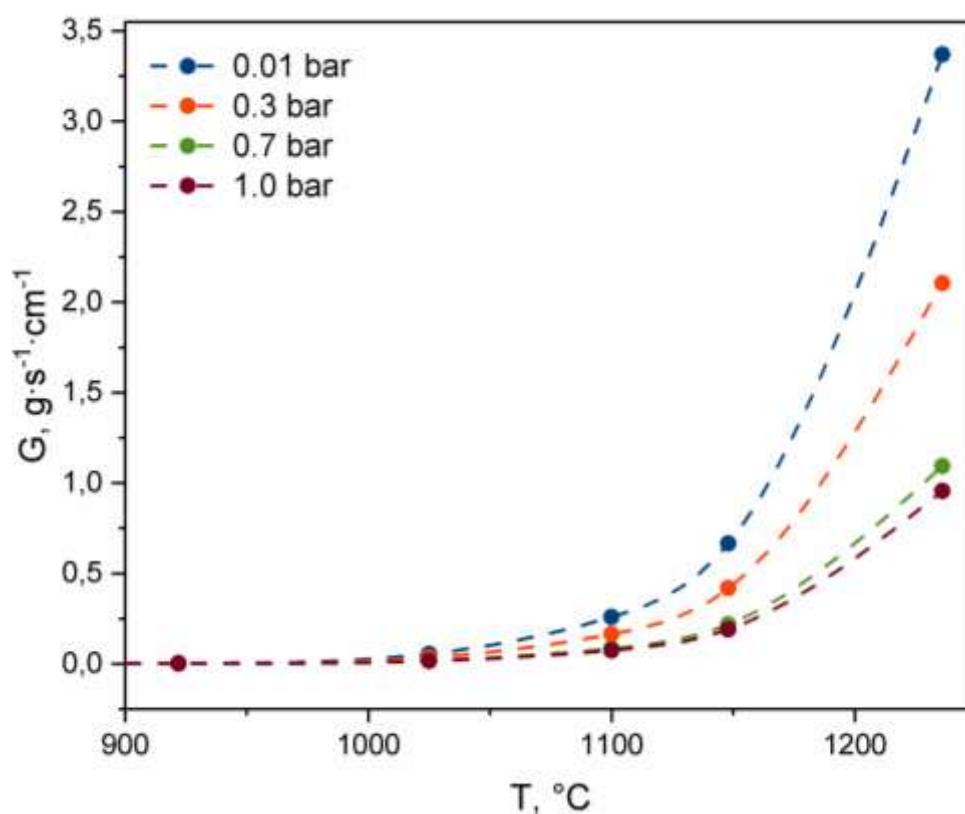


Figure 6 – Dependence of the  $\text{AlF}_3$  sublimation rate on the pressure and temperature

Experimental verification of possibility of silicon CVD by the proposed technology was firstly carried out for the middle investigated synthesis temperature  $1000 \text{ }^\circ\text{C}$  to examine Si yield from chamber pressure (fig. 7b, inset). The highest gas phase pressure (0.5 bar) was selected regarding the beginning of slight silicon fluoridation. As expected from thermodynamic simulation, experiment verifies that with the chamber pressure decrease the reaction yield rises. It is definitely connected with both the growth of the  $\text{AlF}_3$  sublimation rate and promotion of the monofluoride formation. Thus, the chamber pressure for the following experiments was set as 0.01 bar.

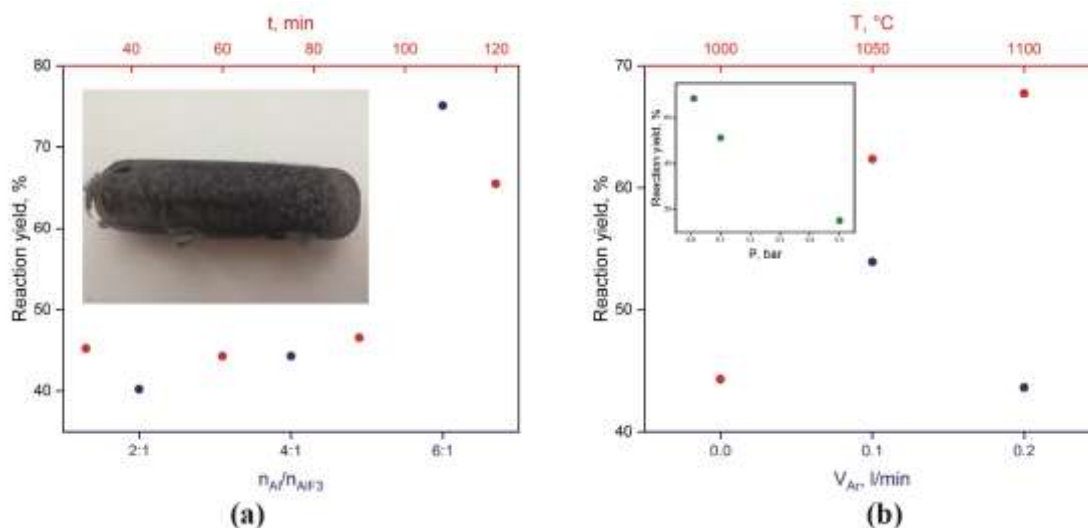


Figure 7 – Dependence of the Si yield **a.** on time of synthesis process and  $n_{Al}/n_{AlF_3}$  molar ratio at 1000 °C and without Ar flow-rate. The experiments with varying  $n_{Al}/n_{AlF_3}$  molar ratio have been carried out during 60 min, the experiments with varying the time of synthesis have been carried out with 4:1  $n_{Al}/n_{AlF_3}$  molar ratio. The photo of Si obtained is shown in the inset. And **b.** On temperature and Ar flow-rate with 4:1  $n_{Al}/n_{AlF_3}$  molar ratio and 60 min time of synthesis process. The experiments with varying Ar flow-rate have been carried out at 1000 °C, the experiments with varying temperature have been carried out without Ar flow-rate. The dependence of Si yield on chamber pressure is shown in the inset.

Both the time of synthesis process and molar ratio  $n_{Al}/n_{AlF_3}$  lead to the increase of silicon yield. Dependences of reaction yield on these parameters are smooth without obvious extremum and demonstrate the similar tendencies (fig. 7a). Obviously, the higher the time of interaction, the higher the target component output. The growth of reaction yield with increase of  $n_{Al}/n_{AlF_3}$  molar ratio is not so evident, but can be explained by gain of degree of interaction of aluminum trifluoride with aluminum.  $AlF_3$  react as transport agent in synthesis mechanism and re-formed at the end of the synthesis. It can re-react with aluminium when it is in excess in system with formation of  $AlF$  and further  $SiO_2$  reduction, what allows one to achieve the highest silicon yield. The synthesis temperature growth results in increase of Si yield, while the dependence of reaction yield from Ar flow-rate is extreme (fig. 7b). Temperature rising enhances the kinetics of processes what is reflected in elevated Si output. The reaction yield with 0.1 l/min Ar flow-rate is higher than such a value for 0 l/min Ar flow-rate, which can be explained by aluminium monofluoride carryover from zone of boat with  $Al/AlF_3$  to boat with  $SiO_2$  by argon flow and, consequently, intensification the interaction between  $AlF$  and  $SiO_2$  by increasing the contact area (fig. 8). The decrease of Si yield with further rising of Ar flow rate-can be caused by more intensive aluminium monofluoride entrainment from reaction zone by the gas flow. Consequently, there is less time for  $AlF$  to react with the  $SiO_2$  with formation of silicon.

Moreover, Ar molecules can partially screen the contact of aluminum monofluoride with silica and reduce kinetic energy of AlF due to impacts with inert argon molecules.



Figure 8 – Photo of Si coated boat after synthesis at **a.** 0 l/min Ar flow-rate and **b.** 0.1 l/min Ar flow-rate

The maximum of the Si yield corresponding to the synthesis conditions  $T = 1100\text{ }^{\circ}\text{C}$ ,  $V_{\text{Ar}} = 0.1\text{ ml/s}$ ,  $P = 0.01\text{ bar}$ ,  $n_{\text{Al}}/n_{\text{AlF}_3}$  molar ratio = 6:1 and  $t_{\text{synthesis}} = 120\text{ min}$  is approximately **97.95 %** from theoretical value.

It can be seen from SEM images (Fig. 9) that Si obtained by the proposed method is formed with dendrites and whiskers morphology and there is no considerable influence of the technological parameters on the morphology. It could be noticed that CVD temperature growth results in average whiskers diameter drop, that could be caused by higher energies of AlF molecules and, consequently, gain of new silicon crystallization centers. An energy dissipation within impacts of aluminum fluoride and inert argon brings the enlargement of silicon grains. Therefore, the finer silicon whiskers are needed the higher the temperature should be maintained.

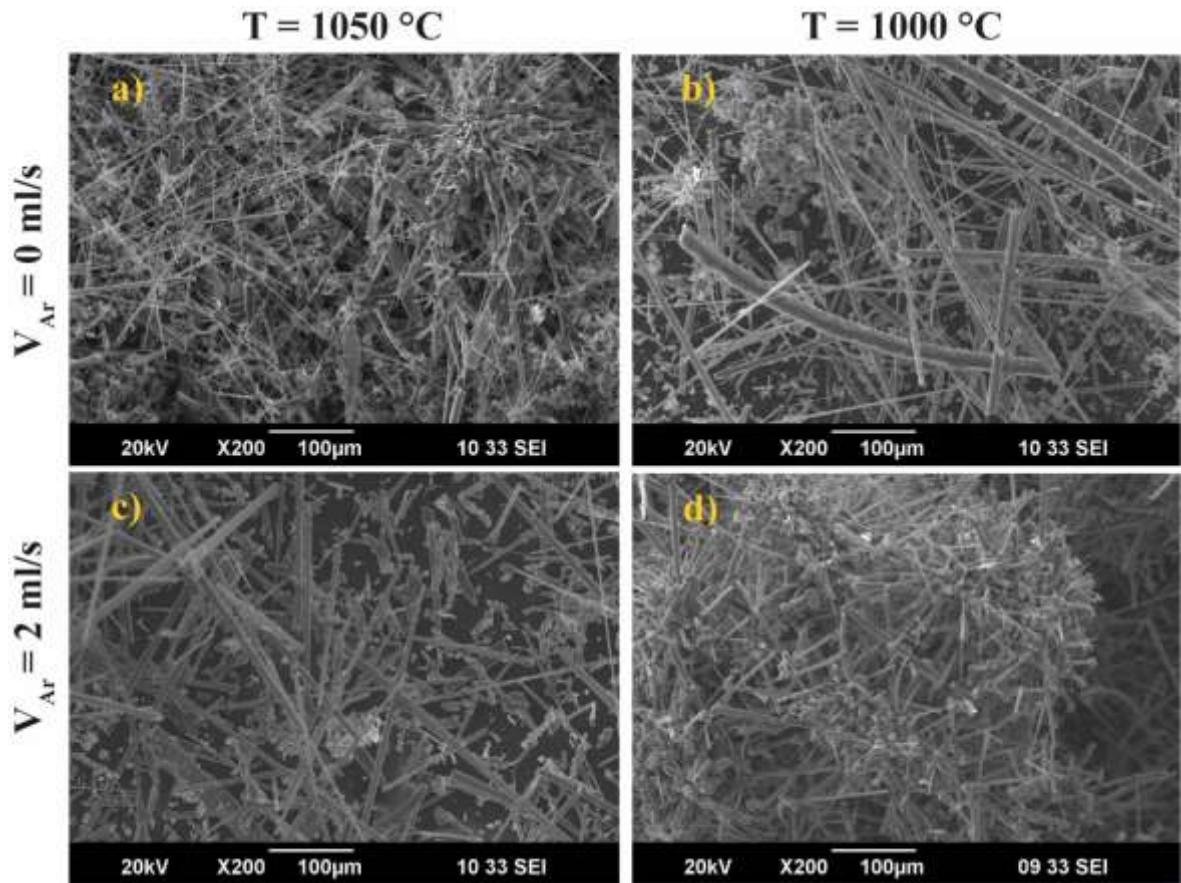
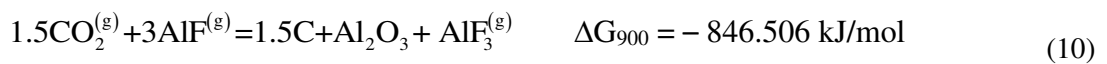


Figure 9 – SEM images of Si dendrites and whiskers obtained under different temperature and argon flow rate conditions

The high-resolution SEM images (Fig 10) shows that obtained Si whiskers have different diameters in 100 nm – 24  $\mu\text{m}$  range. The side faces are not smooth and have styling defects. It was shown in numerous works [24-30], that nanowires morphology is benefit for anode Si materials due to capability to facilitate axial charge transfer, as well as shorten radial  $\text{Li}^+$  ion diffusion distance as the cause of the one-dimensional character.

So, according to the thermodynamical calculations the proposed technology can be adopted for production of Si anode materials, moreover the mechanism of proposed synthesis method can be improved for one-stage production of Si/C composite by using  $\text{CO}_2$  in process as C source, for example (10). That could be suggested as a prospective  $\text{CO}_2$  utilization technology, but a more detailed thermodynamic analysis with consideration of the interaction between all components of investigated system is needed to be done.





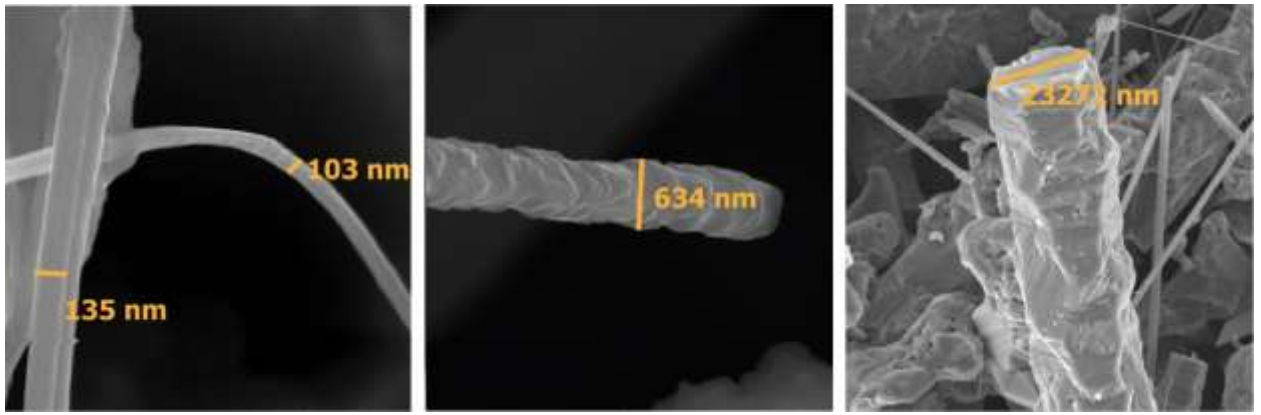


Figure 10 – High-resolution SEM images of the obtained Si whiskers

It was observed, that a sample obtained at  $T = 1100\text{ }^{\circ}\text{C}$ ,  $P = 0.01\text{ bar}$ ,  $V_{\text{Ar}} = 0\text{ ml/sec}$  demonstrates the small content of  $\text{AlF}_3$  impurity (fig. 11a). Also, aluminum trifluoride presence confirmed by XRD (fig 12b). The obtained data allows one to conclude some features in the dependence of the synthesis product phase composition on technological parameters:

- a. Temperature growth results in decreasing of the  $\text{AlF}_3$  impurity content in the synthesized silicon. The aluminum trifluoride condensation point in vacuum is about  $800\text{ }^{\circ}\text{C}$ . As there is a temperature gradient along the tube reactor, the zone of  $\text{AlF}_3$  condensation shifts of the to the low-temperature area at reactor outlet with temperature increasing. So, when the temperature is  $1000\text{ }^{\circ}\text{C}$ , the part of  $\text{AlF}_3$  is deposited directly on the synthesis products, while temperature increasing up to  $1050\text{ }^{\circ}\text{C}$  eliminates these effects. Moreover, aluminum trifluoride starting amount as well as synthesis parameters plays significant role in the Si contamination. If the  $\text{AlF}_3$  remains in the boat at the end of the synthesis cycle it could continue to sublime and deposit during the cooling of the chamber. Thus, the condensation zone shifts along the quartz tube to the center, where Si whiskers are. Such an issue could be solved by varying the synthesis time or the amount of initial material.
- b. Argon flow-rate growth leads to the decrease of synthesis products contamination by  $\text{AlF}_3$  impurity. It can be result of the entrainment of the gaseous  $\text{AlF}_3$  formed in reaction 2 from zone of Si whiskers growth by Ar flow.
- c. At the same time argon flow-rate rise results in the  $\text{SiO}_2$  impurity concentration growth. First, the purity of Ar used is 99.998%, so the oxygen impurities can oxidize the Si. The additional Ar purification by passing gas flow through active metal (Zr, Ti, Mg etc) shavings could prevent the issue. Second, the screening the AlF molecules and dissipation its kinetic energy by impacting with inert argon causes the suppression of

reaction (6). Consequently, in conditions of aluminum monofluoride deficiency, the following reaction (11) can take place. As the result the silica traces could be observed.

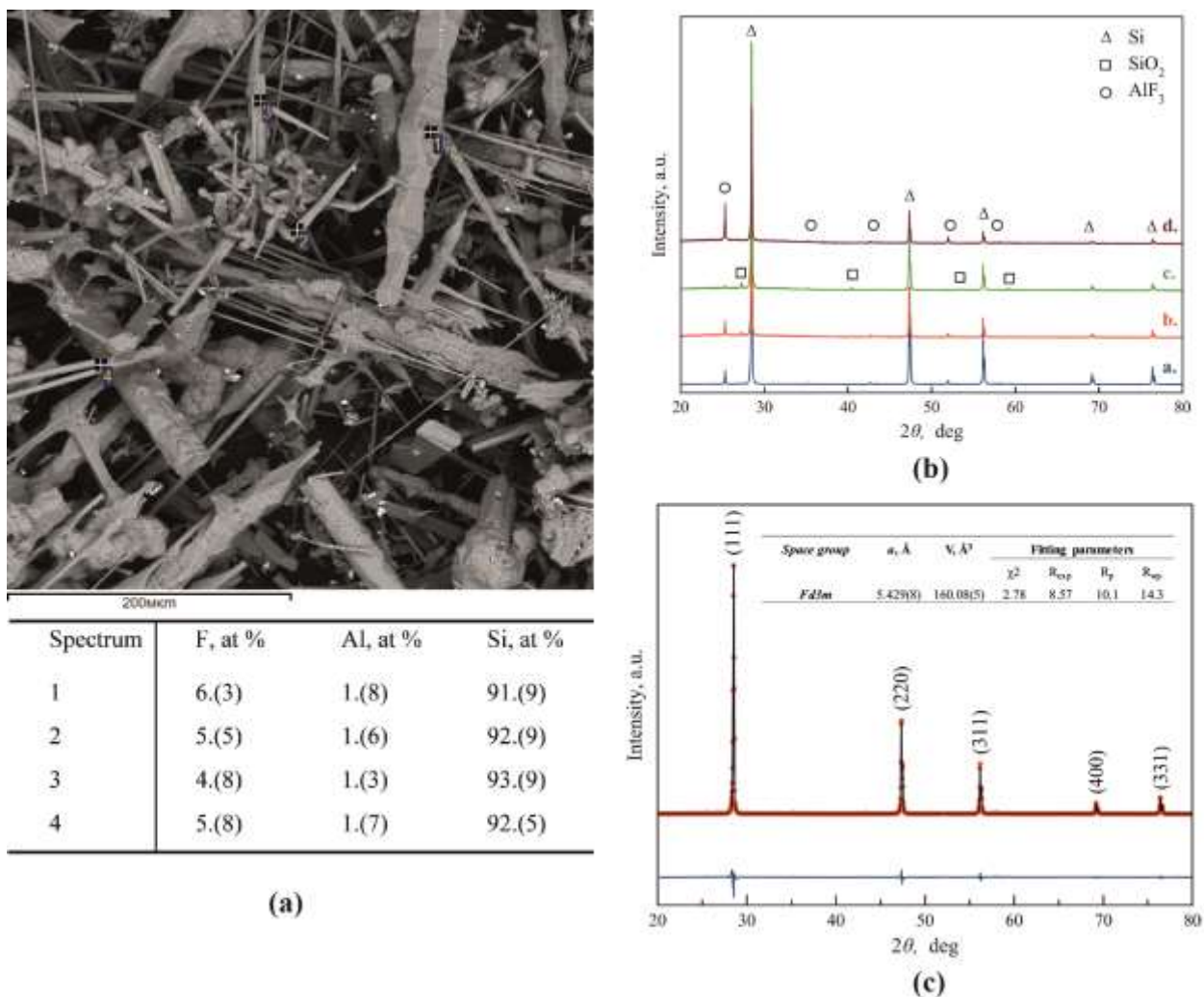
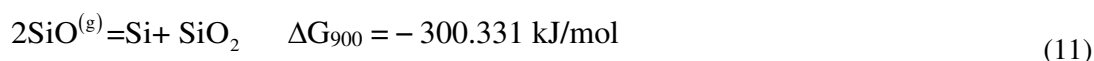


Figure 11 – **a.** EDS of synthesized silicon whiskers; **b.** XRD patterns of Si samples obtained under the following parameters: *a.* 1050 °C and 0 ml/sec Ar flow-rate; *b.* 1000 °C and 2 ml/sec Ar flow-rate; *c.* 1050 °C and 2 ml/sec Ar flow-rate; *d.* 1000 °C and 0 ml/sec Ar flow-rate; **c.** Rietveld refinement of the Si after purification XRD spectra: experimental (red dots), calculated (black line) and difference (blue line)

The XRD pure silicon whiskers were prepared by heating of the synthesis products up to the 1000 °C at vacuumed tube reactor. The  $\text{AlF}_3$  impurity removed due to its sublimation. The Rietveld refinement of as-prepared Si XRD pattern corresponds to the one phase Si with cubic *Fd3m* structure with  $a = 5.429(8) \text{ \AA}$ , which is in good agreement with PDF № 78-2500 (Fig 11c).

#### 4. Conclusion

The Si dendrites and whiskers can be obtained by interaction of gaseous AlF with SiO<sub>2</sub>. It was proposed that the silicon CVD is a multistep chemical process with formation of gaseous SiO and its reaction with AlF. The CVD could be carried out in the range of temperatures 900-1100 °C at the gas phase pressure 0.01-0.1 bar. Such range determines by beginning of active aluminum monofluoride formation and silicon fluodization (1100 °C). The aluminum trifluoride sublimation rate is strongly determined by both the gas phase pressure and the temperature. As the result, the reaction yield significantly depends on such technological parameters as temperature, molar ratio of initial compounds, time of synthesis, transport gas flow-rate, reactor chamber pressure and reaches the 97.95% value. The maximum of Si yield is observed as result of synthesis at T = 1100 °C, V<sub>Ar</sub> = 0.1 ml/s, P = 0.01 bar, n<sub>Al</sub>/n<sub>AlF<sub>3</sub></sub> molar ratio= 6:1 and t<sub>synthesis</sub>= 120 min. Due to AlF screening by argon and AlF<sub>3</sub> depositing such impurities as silica or aluminum trifluoride could be observed in the final product. The as-synthesized Si product requires the additional stage of purification from AlF<sub>3</sub> impurity to solve the issue by heating up to the 1000 °C at vacuumed reactor. But further technology development by creating a controlled temperature gradient along the reactor can exclude this stage.

Si crystals obtained by the proposed CVD method is formed with dendrites and whiskers morphology with different diameters in 100 nm – 24 μm range. There is no considerable influence of the examined technology parameters on the morphology of the Si but there is a slight effect of temperature and argon flow rate on the geometrical sizes of the whiskers. The obtained data shows perspectives for adaptation of the proposed technology for production of Si anode material; moreover, the mechanism of proposed synthesis method can be improved for one-stage production of Si/C composite by using CO<sub>2</sub> in process as C source as well as development of a novel CO<sub>2</sub> utilization technology.

#### Funding

Financial support from Council for grants of the President of Russian Federation (grant no. MK - 182.2022.1.3) is gratefully acknowledged. Authors also appreciate the support of this work within the government assignment № AAAA-A19-119110190048-7.

#### Conflicts of interest

The authors declare no competing interests.

#### Author Contributions Statement

**V.S. Kudyakova:** Formal analysis, Visualization, Writing – original draft, Project administration, Resources. **E.M. Vagizova:** Data curation, Investigation, Methodology. **R.A. Shishkin:** Data curation, Methodology, Supervision, Visualization, Writing – review & editing.



### **Data Availability Statements**

The datasets generated during and/or analyzed during the current study are available from the corresponding author on reasonable request.

### **Ethics approval**

Not applicable (The results of this study do not involve any human or animal).

### **Consent to participate**

Not applicable (The results of this study do not involve any human or animal).

### **Consent for publication**

Not applicable (The results of this study do not involve any human or animal).

## References

- [1] Canham L (2014) Handbook of Porous Silicon. Springer International Publishing.
- [2] Shen X, Tian Z, et al. (2018) J. Energy Chem. <https://doi.org/10.1016/j.jechem.2017.12.012>
- [3] McDowell MT, Lee SW, et al. (2013) Nano Lett. <https://doi.org/10.1021/nl3044508>
- [4] Liu XH, Zhong L, et al. (2012) ACS Nano. <https://doi.org/10.1021/nn204476h>
- [5] Zhao J, Wei W, et al. (2022) ChemPhysChem. <https://doi.org/10.1002/cphc.202200233>.
- [6] Yang Y, Zhang X, et al. (2022) J. Alloys Compd. <https://doi.org/10.1016/j.jallcom.2022.165212>
- [7] Chan CK, Ruffo R, et al. (2009) J. Power Sources. <https://doi.org/10.1016/j.jpowsour.2008.12.047>
- [8] McDowell MT, Lee SW, et al. (2011) Nano Letters. <https://doi.org/10.1021/nl202630n>
- [9] Zhuo Y, Sun H, et al. (2021) Electrochim. Acta. <https://doi.org/10.1016/j.electacta.2021.138522>
- [10] Chan CK, Ruffo R, et al. (2009) J. Power Sources. <https://doi.org/10.1016/j.jpowsour.2008.12.047>
- [11] Chan CK, Peng H, Liu G, et al. (2008) Nat. Nanotechnol. <https://doi.org/10.1038/nnano.2007.411>
- [12] González Z, Chiu HC, Gauvin R, et al. (2022) Mater. Today Commun. <https://doi.org/10.1016/j.mtcomm.2022.103158>
- [13] Ren Y, Yin X, et al. (2022) Chem. Eng. J. <https://doi.org/10.1016/j.cej.2021.133982>
- [14] Xiao Y, Hao D, et al. (2013) ACS Appl. Mater. Interfaces. <https://doi.org/10.1021/am302731y>
- [15] Peng K, Jie J, et al. (2008) Appl. Phys. Lett. <https://doi.org/10.1063/1.2929373>
- [16] Cui L-F, Ruffo R, et al. (2009) Nano Lett. <https://doi.org/10.1021/nl8036323>
- [17] Wen Z, Lu G, et al. (2013) Electrochem. commun. <https://doi.org/10.1016/j.elecom.2013.01.015>
- [18] Wu H, Chan G, et al. (2012) Nature Nanotech. <https://doi.org/10.1038/nnano.2012.35>
- [19] Kulova TL, Skundin AM, Chem Biochem Eng Q, 21, 83–92.
- [20] Kulova TL, Skundin AM, et al. (2007) J. Electroanal. Chem. <https://doi.org/10.1016/j.jelechem.2006.07.002>
- [21] Im J, Kwon JD, et al. (2022) Small Methods. <https://doi.org/10.1002/smt.202101052>
- [22] Bensalah N, Kamand FZ, et al. (2019) Thin Solid Films. <https://doi.org/10.1016/j.tsf.2019.137516>
- [23] He Y, Yu X, et al. (2011) Adv. Mater. <https://doi.org/10.1002/adma.201102568>

- [24] Demirkan MT, Trahey L, Karabacak T (2015) J. Power Sources. <https://doi.org/10.1016/j.jpowsour.2014.09.027>
- [25] Uehara M, Suzuki J, *et al.* (2005) J. Power Sources. <https://doi.org/10.1016/j.jpowsour.2005.03.097>
- [26] Chen LB, Xie JY, *et al.* (2009) J. Appl. Electrochem. <https://doi.org/10.1007/s10800-008-9774-1>
- [27] Schei A, Tuset JKr, Tveit H. (1998) Production of high silicon alloys. Trondheim, Tapir Forlag,
- [28] Pizzini S (2010) Sol. Energy Mater. Sol. Cells. <https://doi.org/10.1016/j.solmat.2010.01.016>
- [29] Chigondo F (2018) Silicon. <https://doi.org/10.1007/s12633-016-9532-7>
- [30] Kasavajjula U, Wang C (2007) J. Power Sources. <https://doi.org/10.1016/j.jpowsour.2006.09.084>
- [31] Kim H, Seo M, Park MH, Cho J (2010) Angew. Chem. Int. Ed. <https://doi.org/10.1002/anie.200906287>
- [32] Huang X, Yang J, Mao S, *et al.* (2014) Adv. Mater. <https://doi.org/10.1002/adma.201400578>
- [33] Ma H, Cheng F, Chen J, *et al.* (2007) Adv. Mater. <https://doi.org/10.1002/adma.200700621>
- [34] Kim G, Jeong S, Shin JH, *et al.* (2014) ACS Nano. <https://doi.org/10.1021/nn406464c>
- [35] Ge M, Lu Y, Ercius P, *et al.* (2014) Nano Lett. <https://doi.org/10.1021/nl403923s>
- [36] Chen S, Bao P, Huang X, *et al.* (2014) Nano Res. <https://doi.org/10.1007/s12274-013-0374-y>
- [37] Xu Y, Yin G, Ma Y, *et al.* (2010) J. Mater. Chem. <https://doi.org/10.1039/B921979J>
- [38] Hanrath T, Korgel BA (2003) Adv. Mater. <https://doi.org/10.1002/adma.200390101>
- [39] Wang N, Zhang YF, Tang YH, *et al.* (1998) Appl. Phys. Lett. <https://doi.org/10.1063/1.122930>
- [40] Meng E, Li W, Nakane K, *et al.* (2013) Phys. Status Solidi C. <https://doi.org/10.1002/pssc.201300347>
- [41] Zhang Y, Zhang Q, Wang N, *et al.* (2001) J. Cryst. Growth. [https://doi.org/10.1016/S0022-0248\(01\)01360-4](https://doi.org/10.1016/S0022-0248(01)01360-4)
- [42] Shishkin RA, Kudryakova VS, Yuferov YuV, Zykov FM (2019) AIP Conf. Proc. <https://doi.org/10.1063/1.5134214>